



SF-10

BEHAVIOR OF REINFORCED CONCRETE BEAM-COLUMN-SLAB SUBASSEMBLAGES SUBJECTED TO BI-DIRECTIONAL LOAD REVERSALS

Kazuhiro KITAYAMA¹, Shunsuke OTANI², and Hiroyuki AOYAMA²

¹Department of Architecture, Utsunomiya University,
Utsunomiya-shi, Tochigi, Japan

²Department of Architecture, University of Tokyo,
Bunkyo-ku, Tokyo, Japan

SUMMARY

Two interior and one exterior beam-column-slab subassemblages were tested under bi-directional cyclic reversed loading. The joint panel region of the three specimens did not fail in shear despite of a high shear stress input. The transverse beams and slabs seemed to have profitable effects on the joint shear resistance. The pinching behavior was observed in load-deformation relations in spite of low bond stress level along beam bars within the joint, and was attributed to the existence of slabs. The entire slab width is regarded as effective at a large deformation. The edge beams, where the slab bars are anchored, must resist torsion induced by the tension forces of slab bars.

INTRODUCTION

The hysteretic behavior of a beam-column joint is influenced by the bond characteristics along beam bars within the joint. An improvement in the bond characteristics makes it possible to develop a good spindle-shape hysteresis with flexural yielding at the critical region at beam ends (Refs.1,2). On the other hand, the bond deterioration yields a pinching hysteresis loop attributable to the pull-out of the beam bars from the joint, and also changes the shear resisting mechanism in the joint to cause shear failure at a large deformation (Refs.2,3). In the past, most of beam-column subassemblages were tested using plane beam-column joints, loaded in one horizontal direction. The beam-column joint in an actual structure is provided with both slabs and transverse beams and is subjected to bi-directional loading under earthquake motions. Therefore, it was decided that three-dimensional beam-column joints with slabs be tested under the bi-directional loading. The main variable was chosen to be the bond conditions along the beam bars within the joint.

EXPERIMENTAL PROGRAM

Specimens Three half-scale three-dimensional reinforced concrete beam-column joints with slabs (called K-series) were tested; two interior joints (Specimens K1 and K2) and one exterior joint (Specimen K3). The column dimensions were 275x275 mm in Specimens K1 and K3, and 375x375 mm in Specimen K2. The beam dimensions were common in the three specimens; 200x300 mm for the longitudinal beams (in the primary loading direction) and 200x285 mm for the transverse beams. The thickness of slabs was 70 mm. Reinforcement details of the specimens are shown in Fig.1. Beam bars of the interior beams passed through the joints,

whereas the top and bottom beam bars of the exterior beam were anchored within the joint. The size of the beam bars was varied in the two interior specimens; D13 bars in Specimen K1 and D10 bars in Specimen K2. The same amount of lateral reinforcement was provided within a joint as that of shear reinforcement required in the middle part of the column in accordance with the AIJ Standard (Ref.4). The slab bars in Specimen K3 parallel to the longitudinal beam were anchored in the transverse beams with 90° hooks. Material properties are listed in Table 1. The ratio of the calculated flexural capacity of column to that of beam, assuming the entire slab width effective to the beam flexural resistance, was 1.40 for Specimen K1, 1.91 for Specimen K2 and 1.85 for Specimen K3.

Table 1 Material Properties

(a) Concrete (unit:kgf/cm ²)			
Specimen	K1,K2	K3	
Compressive Strength			
to the slab	244	199	
above slab	266	196	
Tensile Strength			
to the slab	17	14	
above slab	18	14	
(b) Steel			
Size	Diameter (mm)	Area (cm ²)	Yield Stress (kgf/cm ²)
D6	6.35	0.32	4010
D10	9.53	0.71	4460
D13	12.7	1.27	4420

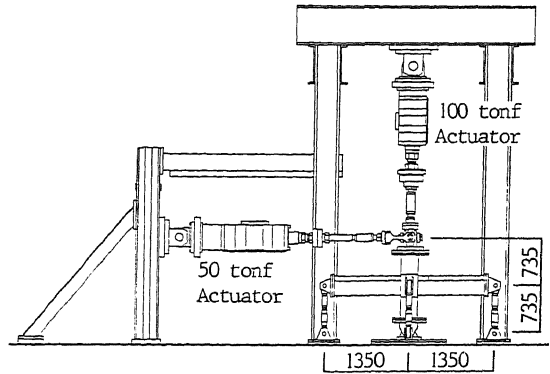
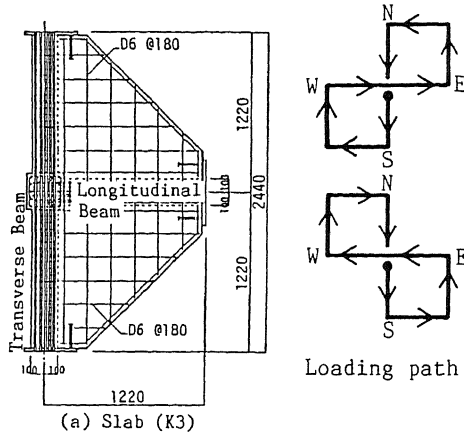
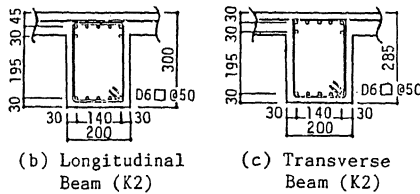


Fig. 2 Loading Apparatus



Specimen	Beam Top Bar	Beam Bottom Bar	Connection ρ_w (%)
K1	4-D13	3-D13	2-D6 4 sets (0.42%)
K2	7-D10	5-D10	2-D6 4 sets (0.33%)
K3	7-D10	5-D10	2-D6 3 sets (0.34%)

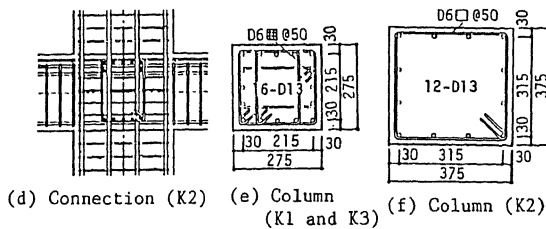


Fig. 1 Reinforcement Details

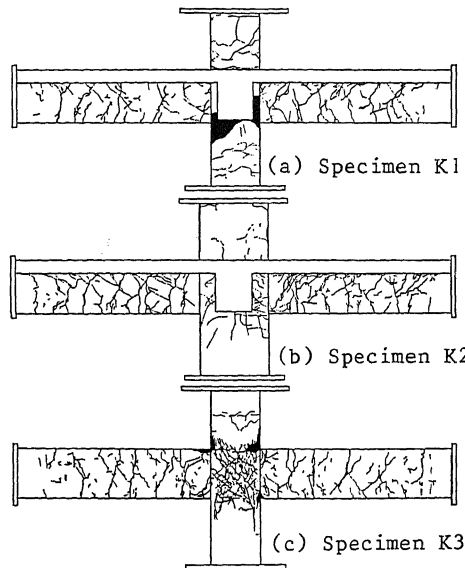


Fig. 3 Crack Patterns after Test

The bond conditions of beam bars was made significantly different in the two interior joint specimens by varying the column width to the beam bar diameter ratio. The bond index is defined as an average bond stress of a beam bar within the joint under simultaneous tensile and compressive yielding assumed at the column faces (Ref.1);

$$u_b = f_y (d_b / h_c) / 2 \quad (1)$$

where f_y : yield strength of a beam bar, d_b : diameter of a beam bar and h_c : column width. The index values are 102 kgf/cm² for Specimen K1 and 57 kgf/cm² for Specimen K2 using the actual yield strength of the beam bar. From these index values, the bond of beam bars in Specimen K1 was expected to be quite severe compared to Specimen K2.

Testing Method The loading apparatus is shown in Fig.2. The constant vertical load of an average axial stress of 20 kgf/cm² and reversing bi-directional horizontal loads were applied at the top of the column. The loading paths under bi-directional loading are shown in Fig.2.

TEST RESULTS

Three specimens developed flexural yielding at the beam ends. The joints did not fail in shear, nor did the transverse beams (edge beams) of Specimen K3 in torsion induced by the tensile forces of the slab bars. The column corner reinforcement of each specimens was observed to yield at a story drift angle as follows; 1/139 rad during the uni-directional loading when the beam bars started to yield in Specimen K1, 1/108 rad during the bi-directional loading after the beam yielding in Specimen K2 and 1/69 rad during the bi-directional loading after the beam yielding in Specimen K3.

Crack Patterns The crack patterns of three specimens observed at the end of loading are shown in Fig.3. Specimen K1 developed a single and wide concentrated crack at the critical section of the beams, exhibiting bond deterioration along the beam reinforcement within the joint, and developed hardly any additional cracks in the beams after a story drift angle of 1/50 rad. The shell concrete spalled in the four corners near and within the joint at a story drift angle of 1/25 rad. On the contrary, Specimen K2 developed fine flexural cracks along the beams after a story drift angle of 1/54 rad. As expected, the bond characteristics along the beam bars within the joint were significantly improved in the joint of Specimen K2 from Specimen K1. Cracks were observed more closely in the slab partially because the beams had to deform more in Specimen K2 with a stiff column. For Specimen K3, torsional cracks were observed in the transverse beams near the column during the loading in the longitudinal direction. But the width was small and the transverse beams did not fail in torsion.

Hysteretic Characteristics The story shear-story drift relations in the longitudinal direction are shown in Fig.4. The story drift angle at yielding was 1/139 rad for Specimen K1 and 1/216 rad for Specimen K2, the difference of which was attributable to the stiffness of the columns. Specimen K2 showed a pinching hysteresis shape under cyclic load reversals although the bond along the beam reinforcement was expected to be good within a joint. The behavior of a three-dimensional beam-column joint and a plane joint is compared using the specimens with comparable bond index values and subjected to comparable loading. The bond index value was 57 kgf/cm² for Specimen K2, and 52 kgf/cm² for Specimen C2 (a plane beam-column joint specimen tested previously, Ref.1). The equivalent viscous damping ratio to quantify the fatness of hysteresis loops was 0.12 for Specimen K2 at a cumulative ductility factor of 35.5 (in the second cycle at a story drift angle of 1/54 rad), and 0.21 for Specimen C2 at a cumulative ductility factor of 37.0 (in the fifth cycle at a story drift angle of 1/46 rad).

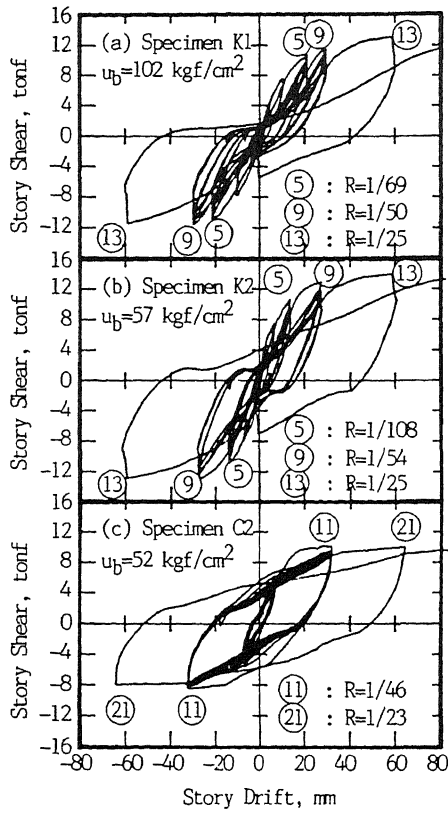


Fig. 4 Story Shear-Drift Relations

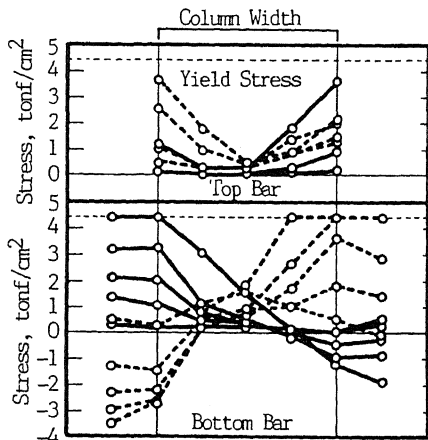


Fig. 5 Stress Distributions along Beam Bar

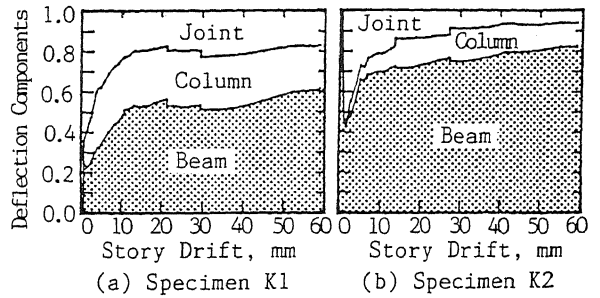


Fig. 6 Deflection Components of Story Drift

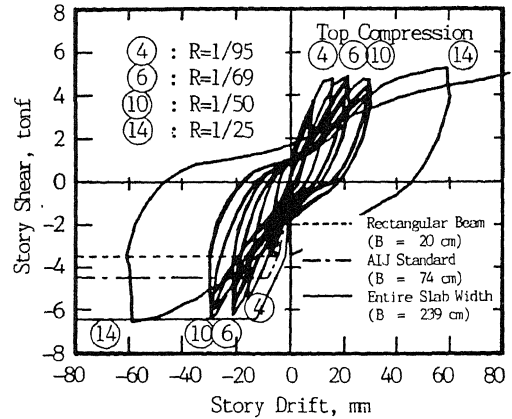


Fig. 7 Story Shear-Drift Relation (Specimen K3)

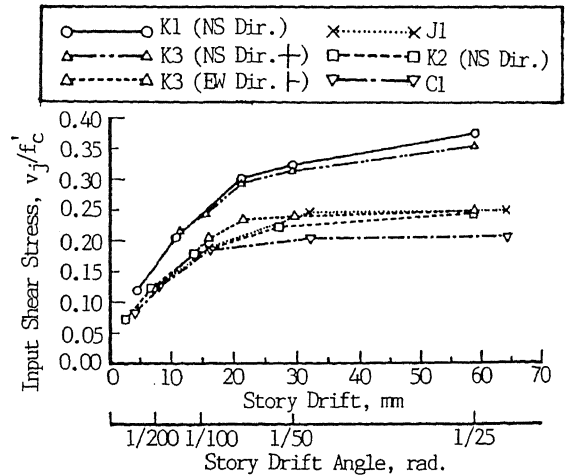


Fig. 8 Shear Stress into Joint

Accordingly, the equivalent viscous damping ratio was considerably smaller in Specimen K2 at a comparable story drift angle and cumulative ductility factor. It is likely that the slab might contribute to the pinching in the shape of hysteresis loops.

Generally, such a pinching hysteresis shape can be observed without bar slip

nor shear failure when the amount of reinforcement differs significantly at the top and bottom of a beam section. The area of the top beam bars was twice the bottom bars in Specimen C2, although the specimen showed a fat spindle shape hysteresis in Fig.4.c. In the test of Specimen K2, ten slab bars were observed to yield and the remaining two slab bars to reach strains above 0.1 % at a story drift angle of 1/54 rad. Therefore, eleven slab bars may well be assumed effective on the beam resistance. Consequently, the total steel area ($= 851 \text{ mm}^2$) of the top beam bars became 2.4 times that of bottom beam bars ($= 357 \text{ mm}^2$), the ratio which is not much different from that of Specimen C2. Therefore, the difference in the amount of the top and bottom reinforcement does not describe the pinching phenomenon of the three dimensional subassemblage.

The stress distribution in the beam top and bottom reinforcement of Specimen K2 are shown in Fig.5 at a story drift angle of 1/216 rad. A solid line represents the distribution during the loading in the positive direction and a broken line in the negative direction. When the bottom beam bar yielded in tension at a connection end, the stress at the other end remained in compression, indicating a good bond of the beam bottom reinforcement within the joint.

On the contrary, the stress along the beam top bar remained in tension over the entire width of the joint. The stress distributed in a V-shape with a minimum stress appearing near the center. Such stress distribution could not be caused by the bond deterioration. It was thought that the location of the neutral axis rised above the beam top reinforcement under positive bending (beam bottom fiber in tension) to yield a tensile stress in the beam top reinforcement at the section. The width of the compression region in the beam critical section appeared to spread widely because of the existence of slabs. Then the location of the neutral axis in the T-shaped beam of Specimen K2 subjected to positive bending was analyzed using the flexural theory, varying the width of the T-section and assuming that plain sections remain plain, and became above the top beam reinforcement in the T-section width greater than 60 cm. Therefore, the entire beam top reinforcement within the joint developed tensile stresses. At the same time, the crack at the beam bottom must open wide to satisfy the compatibility of strains in the section. Hence, the closing of the flexural crack at the beam critical section was delayed when the load was reversed, causing the pinching behavior in Specimen K2.

Displacement Contribution The contribution of parts of Specimens K1 and K2 to the story drift was estimated and shown in Fig.6. The contribution of parts of Specimen K3 in the transverse direction was similar to that of Specimen K1. The contribution of the beam-column joint panel deformation was calculated as the total deflection less the contribution from the beam and column deflections. An abrupt increase in this ratio generally identifies the mode of failure corresponding to the deformation. The ratio of the joint deformation in the three specimens remained almost constant to a story drift angle of 1/25 rad. In other words, the joint panel did not fail in the three specimens. The deflection of beams for Specimen K2 reached 80 % of the total story drift in contrast with 60 % for Specimen K1. The difference in the beam contribution was caused by the difference in the stiffness of the columns.

Effective Width of Slab in Specimen K3 The story shear-story drift relation in the longitudinal direction of Specimen K3 is shown in Fig.7 with story shear resistances calculated varying the cooperating slab widths. In a small story drift range, the stiffness was observed similar to the one calculated with no cooperating slab width. The resistance at a story drift angle of 1/69 rad was observed almost equal to the value calculated with the entire slab width. The slab reinforcement in the entire slab width can contribute to the flexural resistance of the longitudinal beams even though the slab may be located only on one side of the transverse beams. The transverse beams must resist torsional moment induced by the anchoring forces of the slab reinforcement.

SHEAR STRESS LEVEL IN JOINT

The maximum shear stress in the joint during the uni-directional loading is normalized by the concrete compressive strength f_c' and is shown in Fig.8 for Specimens K1, K2, K3 and for plane beam-column joint specimens J1(Ref.3) and C1(Ref.1). The effective joint area to resist shear is defined as the column depth multiplied by the average of the beam and column widths. Specimen J1, in which the maximum shear stress reached $0.25 f_c'$, failed in joint shear at a story drift angle greater than $1/25$ rad after beam flexural yielding. On the other hand, the shear stress reached as high as $0.37 f_c'$ and $0.35 f_c'$ in Specimens K1 and K3 (in the transverse direction), respectively, without failing in the joint. The orthogonal beams framing into the joint and the slabs appeared to confine the joint core concrete although the flexural cracks might remain open in the orthogonal beams at the column faces. The reinforcing bars in the orthogonal beams appear to restrain the opening of internal cracks of the joint core concrete. The strains parallel to the loading direction in the joint lateral reinforcement are shown in Fig.9 for Specimen K2 at a story drift angle of $1/92$ rad and for Specimen C1 of a comparable plane beam-column joint at the input shear stress of approximately $0.18 f_c'$. The strains in Specimen K2 was about half of those in Specimen C1. The width of diagonal shear cracks in the joint core must have been restrained by the beams normal to the loading direction.

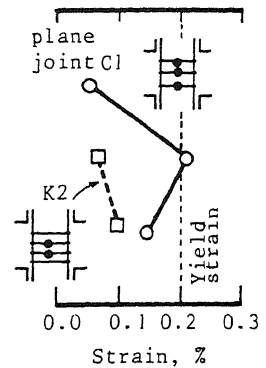


Fig. 9 Strains in Joint Lateral Reinforcement

CONCLUDING REMARKS

From the test results, the following conclusions were drawn;

- 1) Three-dimensional specimens did not fail in joint shear despite a high shear stress level in the connection, probably because the orthogonal beams and slabs enhanced the joint shear capacity.
- 2) The interior beam-column subassemblage with slabs, provided with good bond characteristics along beam bars within the joint, showed a pinching behavior, which may be caused by the delay in crack closing attributable to shift in the location of the neutral axis above the beam top bars under positive loading.
- 3) The slab width, contributing to the beam flexural resistance, spreads with beam deformation. The entire slab width needs be regarded effective at a large deformation. The edge beam, where the slab reinforcement is anchored, must be designed to resist torsional moment exerted by the tension forces of slab reinforcement in the entire width.

REFERENCES

1. Kitayama, K., Kurusu, K., Otani, S. and Aoyama, H., "Behavior of Beam-Column Connections with Improved Beam Reinforcement Bond," Transaction of The Japan Concrete Institute (JCI), Vol.7, 551-558, (1985).
2. Paulay, T. and Park, R., "Joints in Reinforced Concrete Frames Designed for Earthquake Resistance," Research Report 84-9, Department of Civil Engineering, University of Canterbury, June, (1984).
3. Kobayashi, Y., Tamari, M., Otani, S., and Aoyama, H., "Experimental Study on Reinforced Concrete Beam-Column Subassemblages(in Japanese)," Transaction of 6th JCI Annual Meeting, 653-656, (1984).
4. Architectural Institute of Japan (AIJ), "AIJ Standard for Structural Calculation of Reinforced Concrete Structures (in Japanese)," revised in 1982.